A Comparison Between Computerized Tomography, Magnetic Resonance Imaging, and Laser Scanning for Capturing 3-Dimensional Data from a Natural Ear to Aid Rehabilitation

Trevor J. Coward, PhD, MPhil[a]/Brendan J. J. Scott, BDS, BSc, PhD, FDSRCS(Ed)[b]/
Roger M. Watson, BDS, MDS, FDSRCS[c]/Robin Richards, BSc, MSc, PhD[d]

Purpose: To compare dimensional measurements on computer images generated from data captured digitally by 3 different methods to those obtained directly from natural ears and ear casts, so as to determine the optimal method of creating a computer-generated ear image. **Materials and Methods:** Magnetic resonance imaging (MRI) was used to obtain 3-dimensional (3D) data images of the normal ears of 14 subjects. Computerized tomography (CT) and laser scanning (LS) were used to obtain 3D data images from stone casts of the same ears. Dimensional measurements were recorded on 2 occasions between anthropometric landmarks on the subjects' natural ears, casts of the ears, and reconstructed ear images obtained by CT, MRI, and LS. The intraclass correlation coefficients and coefficients of repeatability were calculated. The means of the 2 measurements for each of the dimensions were analyzed using 2-way analysis of variance to determine whether there were differences between the methods of data collection. **Results:** The intraclass correlation coefficients indicated that dimensions could be reliably measured on the natural ears, casts, and CT, MRI, and LS images. The coefficients of repeatability were all of a small magnitude in relation to the overall dimensions studied. No statistical differences existed between the various sources of data (P = .866) (ie, direct, cast, CT, MRI, and LS). **Conclusion:** The 3 methods of imaging have generally resulted in dimensional measurements on the reconstructed images that are similar to those of the original source. These are considered appropriate for manufacturing 3D models that can be used to fabricate a prosthesis. However, other factors may also be important, such as shape, contour, and internal form, and these require further investigation. *Int J Prosthodont 2006;19:92–100.*

Rehabilitation for a patient wishing to disguise the absence of all or part of an ear is achievable with either reconstructive surgery or prosthetic rehabilitation.[1,2] Whichever treatment is selected, dimensional measurements of the existing normal ear and its position, level, and prominence are needed to plan the siting and shaping of the reconstructed ear or prosthesis.[3–6]

Traditionally, direct measurement (anthropometry) has been used to assess the dimensions, location, inclination, and level of an ear on the normal side, which is then used to fabricate a prosthetic ear for the abnormal side. However, there are problems with this approach. The dimensional measurements can be prone to inaccuracy, either because of distortion of the soft tissues of the natural ear or from difficulties in locating landmarks.[7] Furthermore, the fabrication of the prosthesis is dependent on the artistry and skill of the maxillofacial technician and their ability to copy the measurements and shape of the normal ear.[8]

[a]Lecturer, Department of Fixed and Removable Prosthodontics, Guy's King's & St. Thomas' Dental Institute, King's College London, England.

[b]Senior Lecturer/Honorary Consultant, Unit of Restorative Dental Care, Clinical Dental Sciences, Dundee Dental School, Dundee, Scotland.

[c]Emeritus Professor of Dental Prosthetics, Department of Fixed and Removable Prosthodontics, Guy's King's & St. Thomas' Dental Institute, King's College London, England.

[d]Senior Research Fellow, Department of Medical Physics and Bio-Engineering, University College London, England.

Correspondence to: *Dr Trevor Coward, Department of Fixed & Removable Prosthodontics, Guy's King's & St Thomas' Dental Institute, King's College London, Denmark Hill Campus, Caldecot Road, London SE5 9RW, England. Fax: +44 (0) 207 346 3775. E-mail: Trevor.coward@kcl.ac.uk*

COPYRIGHT © 2005 BY QUINTESSENCE PUBLISHING CO, INC.
PRINTING OF THIS DOCUMENT IS RESTRICTED TO PERSONAL USE ONLY.
NO PART OF THIS ARTICLE MAY BE REPRODUCED OR TRANSMITTED IN ANY FORM
WITHOUT WRITTEN PERMISSION FROM THE PUBLISHER.

In the last few years there has been a particular focus on the use of noncontact techniques involving imaging of the ear as a means of producing an appropriately shaped and located prosthesis.[9–14] Wax ears can be produced from computerized tomography (CT), magnetic resonance imaging (MRI), and laser scan (LS) data.[6,8,13–16] However, there have been no comparative studies to determine whether these imaging procedures result in dimensionally accurate auricular prostheses. In previous work, an object of standardized shape and form of similar maximum dimension to a human ear was scanned by the 3 techniques of CT, MRI, and LS.[17] A comparison of the dimensional measurements on the computer-generated images showed no major differences between each technique. Furthermore, the dimensional measurements on the images were very similar to those of the object itself. This suggested that it might be possible to compare such imaging techniques in the production of an auricular prosthesis.

The production of an auricular prosthesis by a rapid prototyping technique is dependent upon having a dimensionally accurate computer-generated image. Errors in the imaging techniques themselves would place limitations on the accuracy of the final model. The purpose of this study was to compare dimensional measurements made on computer-generated ear images from CT, MRI, and LS.

The natural ear itself has a more complex shape and internal form than a standardized cube used as an experimental model. Differences between dimensional measurements on the computer image of the ear generated by each technique might be accounted for, not only by the type of scanning process but also in the ability of the operator consistently to identify landmarks to make the measurements. In the first part of this series of experiments it was necessary to determine whether dimensional measurements of normal ears, ear casts, and the 3-dimensional (3D) reconstructed ear images of several subjects could be reliably measured by 1 operator. In the second part of this series of experiments the dimensional measurements were used to determine if there was an optimal method of obtaining 3D data to create a computer-generated ear image.

Materials and Methods

Sixteen patients with hemifacial microsomia were referred for rehabilitation with an implant-supported auricular prosthesis. Two of the patients were omitted from the study, as they could not fulfill the requirements of the scanning criteria. This was principally because 1 patient had a cardiac pacemaker and the other had ferrometallic clips in the jaw. Both conditions are contraindications for an MRI scan, and these patients were therefore excluded from the study. The study was undertaken on 14 subjects (8 male, 6 female) with hemifacial microsomia who had normally developed facial form on 1 side and abnormally developed facial form on the other. They had an age range of 9 to 61 years (mean age 27 years, 3 months; SD = 14 years, 2 months). All measurements and procedures were carried out on the side of the face with normal facial form and ear structure. Ethical approval was given by the Research Ethics Committee, King's Healthcare NHS Trust.

Identification of Landmarks and Dimensions

Six standard anthropometric landmarks and 3 new landmarks on the side of the head were used to record 6 dimensional measurements: length, width, insertion length, and 3 protrusive measurements of the ear. In this study, the same 6 standard anthropometric landmarks and 3 additional landmarks as defined by Coward[15] were used to record 6 dimensional measurements: length (sa-sba), width (pa-pra), insertion length (obs-obi), and 3 protrusive measurements (sa-sa1, pa-pa1, and sba-sba1) (Tables 1 and 2, Figs 1a and 1b).

Direct Measurement of Natural Ear

The 9 anthropometric landmarks were identified on the natural ear of each patient, and digital sliding calipers (Mitutoyo, Measurement Technology) were employed to measure the 6 dimensions. Two separate measurements were recorded for each dimension at intervals of not less than 1 month.

Cast Production and Measurement

The casts of the natural ears were obtained using an impression technique considered by Coward[15] to be the most acceptable because of clinical handling, surface detail of the cast, and clinical comfort. A Class II stone (Velmix, Kerr) was used for each pour. The 9 anthropometric landmarks were identified on the cast of each patient. Digital sliding calipers were employed to measure the dimensions of length, width, separation of the upper and lower insertion points, and the 3 protrusive measurements on the cast. Two separate measurements were recorded for each dimension at intervals of not less than 1 month.

Scanning Procedures

A CT scanner (Somatom Plus 4, Siemens Bracknell) was used to obtain a 3D image of a stone cast of the subjects' ears. Typically, the scans of each subject's cast were acquired using a 1-mm feed with a rotation

COPYRIGHT © 2005 BY QUINTESSENCE PUBLISHING CO, INC.
PRINTING OF THIS DOCUMENT IS RESTRICTED TO PERSONAL USE ONLY.
NO PART OF THIS ARTICLE MAY BE REPRODUCED OR TRANSMITTED IN ANY FORM
WITHOUT WRITTEN PERMISSION FROM THE PUBLISHER.

Table 1 Six Standard and 3 New Anthropometric Landmarks

Landmark	Location of landmark
Superaurale (sa)	Highest point on the free margin of the auricle
Subaurale (sba)	Lowest point on the free margin of the earlobe
Preaurale (pra)	Most anterior point of the ear located just in front of the helix attachment
Postaurale (pa)	Most posterior point on the free margin of the ear
Otobasion Superius (obs)	Point of attachment of the helix in the temporal region; determines the upper border of ear insertion
Otobasion Inferious (obi)	Point of attachment of the earlobe to the cheek; determines the lower border of the ear insertion
New Point (sa1)	Point on side of the head orthogonal to the highest point on free margin of the top of ear (sa)
New Point (pa1)	Point on side of head orthogonal to the most posterior point on the free margin of the ear (pa)
New Point (sba1)	Point on side of head orthogonal to lowest point on free margin of the ear (sba)

Table 2 Dimensional Measurements of the Ear

Dimension	Description
sa-sba	Length of ear
pa-pra	Width of ear
obs-obi	Insertion length of ear
sa-sa1	Protrusive measurement from top of ear to point orthogonal to head
pa-pa1	Protrusive measurement from most posterior point on helix to point orthogonal to head
sba-sba1	Protrusive measurement from lowest point on free margin of lobe to point orthogonal to head

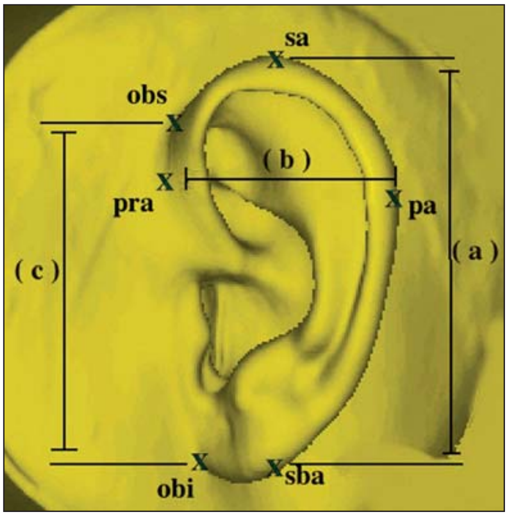

Fig 1a *(left)* Anthropometric landmarks used to record the dimensions of length, width, and insertion length of the ear. X indicates each individual anthropometric landmark.

Fig 1b *(right)* Anthropometric landmarks used to record the dimensions of protrusion. X indicates each individual anthropometric landmark.

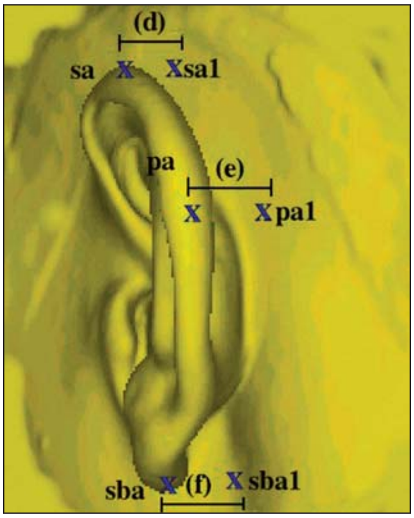

time of 0.75 seconds and a space between slices of 1 mm. This allowed the data to be reconstructed as 1-mm slices (Table 3).

The same stone casts of the 14 subjects' normal ears were laser scanned. Each scan consisted of approximately 240 vertical profiles obtained at 0.5-degree increments, with each profile containing approximately 151 to 176 points (Table 3).

In the first instance, an attempt was made to scan plaster casts of the ear using MRI. Two MRI sequences (dual-echo steady state [DESS] and T1-weighted spin-echo sequences), were applied (Table 4). To achieve a signal, these casts were submerged in water and supported on a bed of agar-agar. A negative image of the water surrounding the ear cast was obtained. The digitized data were fed into the computer software program, which inverted the 3D data to produce a positive image of the ear. During these experiments it became apparent that MRI scanning of the ear cast could not provide consistent digitization and therefore it became necessary to also perform an MRI scan of each subject's natural ear.

At present there is no set MRI scanning sequence to obtain the image of the external human ear. It was nec-

COPYRIGHT © 2005 BY QUINTESSENCE PUBLISHING CO, INC.
PRINTING OF THIS DOCUMENT IS RESTRICTED TO PERSONAL USE ONLY.
NO PART OF THIS ARTICLE MAY BE REPRODUCED OR TRANSMITTED IN ANY FORM
WITHOUT WRITTEN PERMISSION FROM THE PUBLISHER.

Table 3 Details of Scanner and Data Acquisition for Each Method of Obtaining 3-Dimensional Data

CT scanning data	LS data
Siemens Somatom Plus 4 Scanner (Siemens Medical)	Low-power Class 3 gallium/indium laser (1 mW) (Bio-Engineering and Medical Physics Department, University College London
KV 120, mA 90	–
Matrix 512 × 512 mm Field of View 100 × 100 mm	TV zoom lens (f ~ 12.7 to 75 mm) operating at 49 mm with a lens aperture of f2.8 mm
44 to 79 slices (depending on ear size)	240 vertical profiles
Slice width 1 mm	Each profile contains 151 to 176 points at increments of approximately 0.5 degrees
Collimation 1 mm	–
AB50	–

Table 4 MRI Sequences Used to Obtain Images of Plaster Casts of Ears

Parameter	DESS	TI-weighted spin echo sequence
TR (ms)	40	500
TE (ms)	6	8.4
Slice width (mm)	2	–
Matrix (mm)	256 × 128	256 × 256
Field of view (mm)	200 × 200	200 × 200
Pixel size (mm)	1.6 × 0.8	0.8 × 0.8
Bandwidth (me)	–	130
Acquisition time (min)	10.57	12.52

Siemens Magnetom Expert 1 Tesla scanner (Siemens Medical) was used.

essary to investigate several sequences to determine an appropriate method of obtaining digitized data suitable for viewing as a reconstructed image. The 3 MRI scanning sequences (Table 5), for acquiring data by continuous axial slices, were visually assessed by examining the reconstructed images on the computer screen. These were DESS, a 2D fast low-angle shot (FLASH) sequence, and a magnetization-prepared rapid acquisition with gradient echo (MP RAGE) sequence. In the definitive scanning sequences on each of the 14 subjects, a DESS sequence was used.

Reconstruction of 3D Data

Two customized computer software programs (developed by University College London, Department of Medical Physics and Bio-Engineering) were used to view the reconstructed images. One program was used to view volumetric data, ie, CT and MRI. The second program reconstructed the surface data obtained from laser scans. Fourteen subjects' ears and faces were MRI scanned, and the ear casts of each subject were also scanned by CT and LS, producing 3D data in a format suitable for viewing on a computer screen as a 3D image (Figs 2a to 2c). When these were displayed, the viewpoints for the reconstructed images of each subject's ear and ear cast were aligned and recorded. This enabled them to occupy matching spatial coordinates on the screen to permit consistent viewing and analysis of the images.

The dimensional measurements on the computer-reconstructed ear images obtained by CT, MRI, and LS were obtained by identifying the anthropometric landmarks with a cursor. The program allowed measurements to be recorded between the identified landmarks. The landmarks were saved as a landmark file and could be retrieved on future occasions. Two measurements were recorded for each dimension at intervals of not less than 1 month.

COPYRIGHT © 2005 BY QUINTESSENCE PUBLISHING CO, INC.
PRINTING OF THIS DOCUMENT IS RESTRICTED TO PERSONAL USE ONLY.
NO PART OF THIS ARTICLE MAY BE REPRODUCED OR TRANSMITTED IN ANY FORM
WITHOUT WRITTEN PERMISSION FROM THE PUBLISHER.

Table 5 MRI Scanning Sequences Used to Obtain Images of the Human Ear

Parameter	DESS	2D FLASH	MP RAGE
TR	19 ms	836 ms	11.4 ms
TE	6 ms	10 ms	4.4 ms
Flip angle	35 deg	60 deg	12 deg
Slice thickness	1 slab 128 mm thick with 128 partitions = 1-mm slices	1 slab 128 mm thick with 64 partitions = 2-mm slices	1 slab 231 mm thick with 160 partitions = 1.41-mm slices
Matrix	192 × 256 mm	192 × 512 mm	160 × 256 mm
Field of view	240 (× 7/8) × 240 mm	400 (× 5/8) × 400 mm	300 (× 5/8) × 188 mm
Acquisition time	7 min 48 s	5 min 26 s	4 min 26 s

A Siemens Magnetom Expert Scanner (Siemens Medical) was used.

Fig 2a Image of ear cast from CT data.

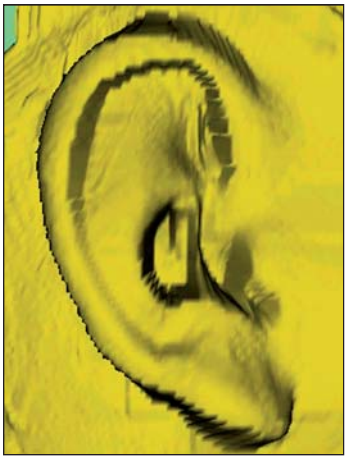

Fig 2b Image of ear cast from LS data.

Fig 2c Image of natural ear from MRI data.

Repeatability

The mean differences were calculated between the 2 measurements that had been recorded at an interval of not less than 1 month apart. In the first part of this series of experiments, it was necessary to determine whether dimensional measurements of normal ears, ear casts, and 3D reconstructed images could be reliably measured by 1 operator. This was achieved by calculating the intraclass correlation coefficients (ICCs) and coefficients of repeatability (CRs) for each of the 6 dimensions studied on the different media (ie, natural ear, cast, MRI, CT, and LS images). The repeatability value (CR) is defined as that below which the absolute difference between 2 single test results, obtained under repeatable conditions, may be expected to lie within a probability of 95%.[18]

Comparison of Dimensional Measurements

The means of the 2 direct measurements for each of the 6 dimensions on the 14 subjects' normal ears were compared to similar measurements recorded from the casts and the images reconstructed from CT, LS, and MRI data. The means and 95% confidence intervals for the 6 dimensional measurements for each source of data were calculated.

Data Analysis

The ICCs were calculated to assess the reliability of the repeated measurements for each dimension. These were assessed for measurements on the natural ears, casts, and CT, MRI, and LS images. The mean of 2 measurements for each of the 6 dimensions (sa-sba, pa-pra, obs-obi, sa-sa1, pa-pa1, & sba-sba1) were analyzed using 2-way analysis of variance (ANOVA) to determine whether there were significant differences between the

COPYRIGHT © 2005 BY QUINTESSENCE PUBLISHING CO, INC.
PRINTING OF THIS DOCUMENT IS RESTRICTED TO PERSONAL USE ONLY.
NO PART OF THIS ARTICLE MAY BE REPRODUCED OR TRANSMITTED IN ANY FORM
WITHOUT WRITTEN PERMISSION FROM THE PUBLISHER.

Fig 3a DESS sequence.

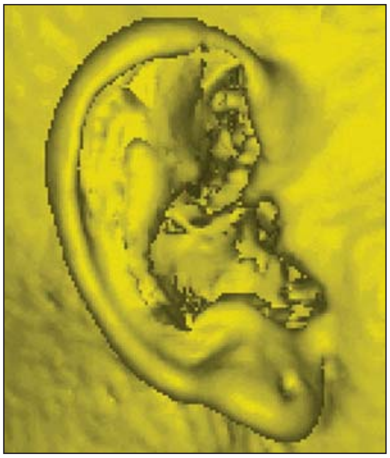

Fig 3b 2D FLASH sequence.

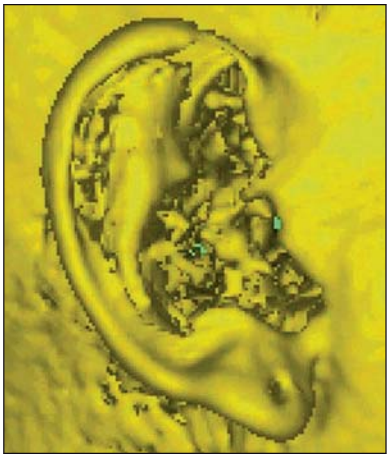

Fig 3c MP RAGE sequence.

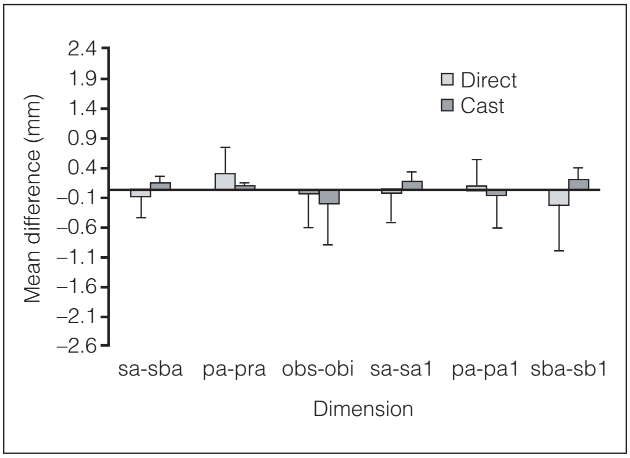

Fig 4a Mean differences between direct ear/ear cast measurement 1 and direct ear/ear cast measurement 2 (error bars represent standard deviations). Each individual bar represents the mean difference between the repeated readings for each dimension on the 14 subjects. The baseline represents no difference between the 2 measurements.

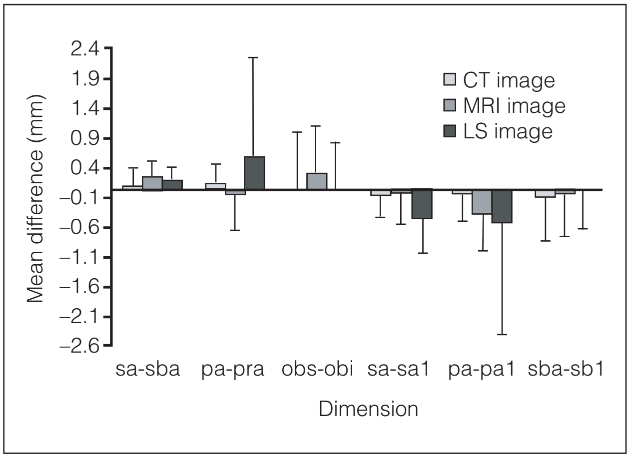

Fig 4b Differences between measurement 1 of reconstructed CT, MRI, and LS images and measurement 2 of reconstructed CT, MRI, and LS images (error bars represent standard deviations). Each individual bar represents the mean difference between the repeated readings for each dimension on the 14 subjects. The baseline represents no difference between the 2 measurements.

different sources of data (ie, direct measurements from the subjects' ears, casts of the ears, and reconstructed images of the ears obtained from CT, MRI, and LS data). Statistical calculations were carried out with SPSS software, Version 11.5.

Results

There were no difficulties encountered in the identification of landmarks on the natural ears of the 14 subjects and the casts. Similarly, landmarks could be located on the computer-generated images from the CT and LS of the cast. However, the MRI sequence was unable to capture an image of the cast with good surface detail and contour. For this reason, it became necessary to carry out the MRI sequence on the natural ear. Visual examination of the reconstructed ear images obtained by the different MRI scanning sequences revealed that the DESS sequence produced an image with the smoothest contours and the fewest artifacts and loss of detail (Figs 3a to 3c).

Repeated Dimensional Measurements

The differences between the 2 measurements for each of the 6 dimensions on the subjects, casts, and the reconstructed images are displayed as mean differences and standard deviations for the 14 subjects (Figs 4a and 4b). The ICCs for the repeated measurements on the natural ears, casts, and reconstructed images are shown in Table 6.

COPYRIGHT © 2005 BY QUINTESSENCE PUBLISHING CO, INC. PRINTING OF THIS DOCUMENT IS RESTRICTED TO PERSONAL USE ONLY. NO PART OF THIS ARTICLE MAY BE REPRODUCED OR TRANSMITTED IN ANY FORM WITHOUT WRITTEN PERMISSION FROM THE PUBLISHER.

Table 6 Intraclass Correlation Coefficients Calculated from the 2 Readings of Each of the 6 Dimensions on the Natural Ears (Direct), Cast, CT, MRI, and LS Images

Method	Intraclass correlation coefficient
Natural ear (direct)	0.99
Cast	0.99
CT image	0.99
MRI image	0.99
LS image	0.99

Table 7a Coefficients of Repeatability (CR) for 6 Dimensional Measurements Recorded on the Ears of 14 Subjects and 14 Ear Casts of the Same Subjects

Dimension	CR for subject (mm)	CR for cast (mm)
sa-sba	0.73	0.70
pa-pra	0.82	0.73
obs-obi	1.16	1.42
sa-a1	1.02	0.54
pa-b1	0.91	1.12
sba-c1	1.55	1.01

Table 7b Coefficients of Repeatability (CR) for 6 Dimensional Measurements Recorded on 14 Reconstructed Images Obtained from CT, MRI, and LS Data

Dimension	CR for CT image (mm)	CR for MRI image (mm)	CR for LS image (mm)
sa-sba	0.59	0.56	0.40
pa-pra	0.68	1.17	3.39
obs-obi	1.96	1.56	1.58
sa-a1	0.69	1.09	1.18
pa-b1	0.86	1.20	3.76
sba-c1	1.44	1.47	1.29

The CRs for each dimension using each measurement technique (natural ear, cast, CT image, MRI image, LS image) are shown in Tables 7a and 7b. Generally, these coefficients were of a small magnitude in relation to the overall dimension studied.

The mean dimensional differences between the casts or reconstructed images compared with the natural ears were very small. Figure 5 shows the means differences and 95% confidence intervals for the major dimensions of the ear (ie, length = sa-sba; width = pa-pra; insertion length = obs-obi). Generally the CT, MRI, and LS images had dimensional measurements that were slightly smaller than those of the the natural ears. The largest differences were in the LS images, with a maximum mean difference of 1.36 mm observed for the dimension of length (LS versus natural ear). Two of the 3 dimensions on the cast (pa-pra and obs-obi) were a little larger than the natural ear.

For all 3 protrusive measurements (sa-sa1, pa-pa1, and sa-sba1), the mean differences between the casts and reconstructed ear images compared to the natural ears were very small (Fig 6). The 3 protrusive dimensions on the casts were a little smaller than those on the natural ears. The dimension sba-sba1 was a little smaller on each of the images than on the natural ear. The dimension sa-sa1 was a little larger on each set of images than on the natural ear. The dimension pa-pa1 was smaller on the CT and LS image but larger on the MRI image compared with the natural ear.

A comparison was made between all measurements for each dimension between the different methods of data collection. The 2-way ANOVA revealed no statistical differences between the various sources of data ($P = .866$) (ie, direct and cast measurements and reconstructed images from CT, MRI, and LS).

Discussion

This study has shown that it is possible to capture data reliably using all imaging techniques, either from a cast of the ear or directly from the scan of the natural ear itself. However, there were some small differences between the techniques in relation to certain dimensional measurements. Although the sample size of 14 subjects might be considered to be modest, the statistical power was found to be greater than 90% for a significance level of $P = .05$ for all dimensions. This was based on a difference value of 2 mm as it was judged that this would be clinically undetectable in subjects. Furthermore, Farkas[4] felt that differences of 5 mm in length would be clinically undetectable. Such differences would mean that even greater power levels would be found than those used in the present study. For this reason, the sample size of 14 subjects was judged to be more than sufficient to compare the methods of scanning.

COPYRIGHT © 2005 BY QUINTESSENCE PUBLISHING CO, INC.
PRINTING OF THIS DOCUMENT IS RESTRICTED TO PERSONAL USE ONLY.
NO PART OF THIS ARTICLE MAY BE REPRODUCED OR TRANSMITTED IN ANY FORM
WITHOUT WRITTEN PERMISSION FROM THE PUBLISHER.

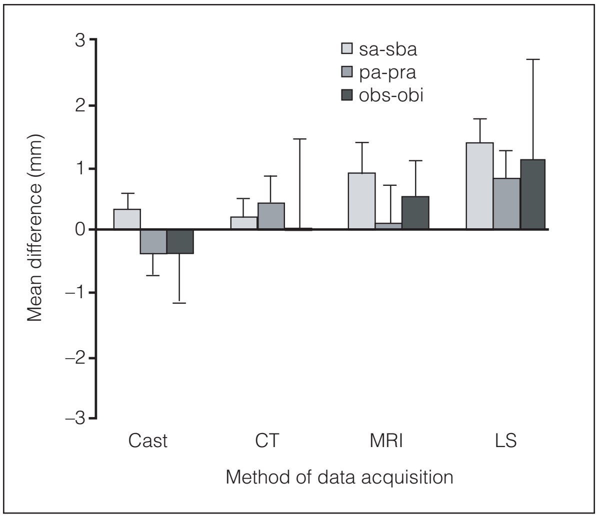

Fig 5 Mean differences between the dimensional measurements of the casts and reconstructed ear images compared with the same dimensions on the natural ear (error bars represent 95% confidence intervals). A negative difference indicates that the dimensional measurements are larger than the natural ear. The baseline represents no difference between the 2 measurements.

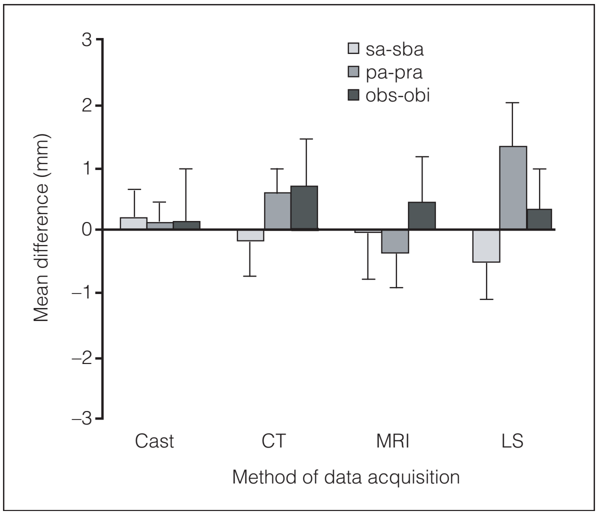

Fig 6 Mean differences between the protrusive dimensional measurements of the reconstructed casts and ear images compared to the same dimensions on the natural ear (error bars represent 95% confidence intervals). A negative difference indicates that the dimensional measurements are larger than the natural ear. The baseline represents no difference betweeen the 2 measurements.

Ideally, a comparison of the different sources of data collection (ie, CT, MRI, and LS) would be best achieved by scanning the subjects' natural ears. However, CT scanning is an invasive technique and it is not considered ethical by some groups of professionals in the United Kingdom to scan a subject solely to obtain an image of, for example, an external ear. For this reason the images generated from CT and LS were taken from the plaster cast.

The technique for producing the cast ensured that there was very little dimensional change from the natural ears. In previous work employing this technique, Coward[15] was able to conclude that the technique resulted in the least dimensional change between the natural ear and cast of the same ear (all dimensions had mean differences of less than 1 mm).

Various MRI scanning sequences were attempted to obtain an image of a plaster cast. It was not possible to obtain a well-defined image from a scan of a plaster cast of an ear because the MRI technique requires hydrogen ions to obtain an image. An MRI scanning sequence suitable for obtaining images of cartilage and synovial fluid (DESS sequence) was therefore utilized to capture images of natural ears. This imaging technique was found to be comparable to digitized data obtained by CT and laser scanning of a cast poured from an impression of a natural ear.

Despite the source of the imaging, there were no difficulties in each of the scanning procedures, and the landmarks could generally be readily located on the reconstructed images. This was confirmed by analysis of the repeated measurements. The data for the repeated measurements on the subjects' ears, casts, and reconstructed images show that the mean differences for the 2 sets of readings were small for each dimension studied. Furthermore, the high values of the ICCs indicated that for all media (ie, natural ear, cast, and CT, MRI, and LS images), the dimensions could be measured reliably. The RC is based on 95% of the differences between the repeated measurements lying within 2 standard deviations of the mean difference.[19] The CRs for all 3D measurements related to the size of the ear (sa-sba, pa-pri, obs-obi) were less than 2 mm for the subjects' ears, casts, and CT- and MRI-reconstructed images. In relation to the LS-reconstructed image, 2 of the 3 CRs were also less than 2 mm. However, for the dimension of width (pa-pra), the CR was 3.39 mm. The data for the LS images compare favorably with previous work.[9] With regard to all protrusive measurements (sa-sa1, pa-pa1, sba-sba1), the CR for the subject's ears, casts, and CT- and MRI-reconstructed images were also less than 2 mm. However, for 1 dimension (pa-pa1) in the LS-reconstructed image, the CR was 3.76 mm.

For most of the dimensions examined, a CR of less than 2 mm represents a small proportion of the overall clinical measurement with respect to the size of each ear (eg, length 49.31 to 72.88 mm, width 32.20 to 44.45 mm, insertion length of ear 41.10 to 63.73 mm). Farkas,[4] when observing ears in normal subjects, reported that a 5-mm difference in length and a 3- to 4-mm difference in width were never visible. It was therefore apparent that the differences observed in this study were unlikely to be clinically obvious, even to a trained observer.

For the protrusive measurements, similarly CRs of less than 2 mm are unlikely to be clinically detectable,

COPYRIGHT © 2005 BY QUINTESSENCE PUBLISHING CO, INC. PRINTING OF THIS DOCUMENT IS RESTRICTED TO PERSONAL USE ONLY. NO PART OF THIS ARTICLE MAY BE REPRODUCED OR TRANSMITTED IN ANY FORM WITHOUT WRITTEN PERMISSION FROM THE PUBLISHER.

although they do represent a larger proportion of the overall protrusive measurement (7.01 to 28.34 mm). The CRs in the LS-reconstructed images that were greater than 2 mm may be accounted for by the difficulty in identifying some of the anthropometric landmarks, owing to less well defined surface detail. However, they are not likely to be clinically observable.

In relation to the dimensions of the ear itself, only small differences were found between either the casts or reconstructed images compared with the direct measurements. The 3 major dimensions of the reconstructed ear image (length, width, and insertion length) obtained by digitized LS data had the greatest differences compared with those on the natural ear. Nevertheless, they were generally of a very small magnitude. These differences may be a reflection of the difficulty in identifying the anthropometric landmarks on LS images. For the 3 dimensions of protrusion (sa-sa1, pa-pa1, and sba-sba1), again, only small differences were found between the dimensions on the natural ears and those on the casts and images.

In comparing the results of the methods by which each of the 6 dimensions were measured, little difference existed. The 2-way ANOVA revealed no statistical differences between the direct measurements of the natural ears, the casts and the CT, MRI, and LS images.

Conclusion

The 3 methods of imaging generally resulted in the dimensional measurements on the reconstructed images being similar to those from the original source (cast or subject themselves). Although there were some differences between the LS images for certain dimensions, these were not statistically significant and are not thought to have any clinical consequence for rehabilitation. The present study has explored a number of dimensions, which can be reproducibly measured, that are used in the construction of auricular prostheses. However, other factors may also be important, such as shape, contour, and internal form, and need to be investigated further. In relation to patients who require rehabilitation of an absent ear, the use of imaging techniques offers the potential to manufacture a 3D model that can be used to fabricate the final prosthesis. Although there are reports of ear prostheses being made using such techniques, there have been no reported comparative studies on the results obtained from various imaging methods.[8,10,13,14,16,20] This requires further study.

Acknowledgments

We acknowledge the generous use of facilities in the Department of Bio-engineering and Medical Physics, University College, London, and the Magnetic Resonance Imaging and Computerised Tomography units at King's College Hospital. Particular thanks are extended to Dr Alf Linney (University College, London), Mrs Janice Mackie, Mr John Totman, and Mr Simon Gover (King's College Hospital).

References

1. Fine L, Robinson J, Barnhart G. Absence or major loss of part of the external ear and its correction. J Prosthet Dent 1974;31:313-322.
2. Wilkes GH, Wolfaardt JF. Osseointegrated alloplastic versus autogenous ear reconstruction: Criteria for treatment selection. Plast Reconstr Surg 1994;93:967-979.
3. Figalova P, Farkas LG. Localization of the auricle by means of anthropometric methods. Acta Chir Plast 1968;10:7-14.
4. Farkas LG. Anthropometry of normal and anomalous ears. Clin Plast Surg 1978;5:401-412.
5. Tolleth H. A hierarchy of values in the design and construction of the ear. Clin Plastic Surg 1990;17:193-207.
6. Watson RM, Coward TJ, Forman GH, Moss JP. Considerations in treatment planning for implant-supported prostheses. Int J Oral Maxillofac Implants 1993;8:445-449.
7. Farkas LG. Anthropometry of the Head and Face in Medicine. New York: Elsevier, 1981.
8. Coward TJ, Watson RM, Wilkinson IC. Fabrication of a wax ear by rapid-process modeling using stereolithography. Int J Prosthodont 1999;12:20-27.
9. Coward TJ, Watson RM, Scott BJJ. Laser scanning for the identification of repeatable landmarks of the ears and face. Br J Plast Surg 1997;50:308-314.
10. Chen LH, Tsutsumi S, Lizuka T. A CAD/CAM technique for fabricating facial prostheses: A preliminary report. Int J Prosthodont 1997;10:467-472.
11. Coward TJ, Scott BJJ, Watson RM, Richards R. Laser scanning of the ear identifying the shape and position in subjects with normal facial symmetry. Int J Oral Maxillofac Surg 2000;29:18-23.
12. Coward TJ, Scott BJJ, Watson RM, Richards R. Identifying the position of an ear from a laser scan: The significance for planning rehabilitation. Int J Oral Maxillofac Surg 2002;31:244-251.
13. Jiao T, Zhang F, Huang X, Wang C. Design and fabrication of auricular prostheses by CAD/CAM system. Int J Prosthodont 2004;17:460-463.
14. Sykes LM, Parrot AM, Owen CP, Snaddon DR. Applications of rapid protyping in maxillofacial prostheses. Int J Prosthodont 2004;17:454-459.
15. Coward TJ. Production of Artificial Ears: Aspects of the Technical Problem [thesis]. London: University of London, 1996.
16. Coward TJ, Watson RM. Use of laser scanning systems in the fabrication of auricular prostheses. Quintessence Dent Technol 1997;20:47-54.
17. Coward TJ, Scott BJJ, Watson RM, Richards R. A comparison between computerised tomography, magnetic resonance imaging, and laser scanning for capturing three dimensional data from an object of standard form. Int J Prosthodont 2005;18:405–413.
18. British Standards Institution. Precision of Test Methods 1. Guide for Determination and Reproducibility for a Standard Test Method (BS 5497 Part 1). London: British Standards Institution, 1979.
19. Bland JM, Altman DG. Statistical methods for assessing agreement between two methods of clinical measurement. Lancet 1986;1(8476):307-310.
20. Cheah CM, Chua CK, Tan KH, Teo CK. Integration of laser surface digitization with CAD/CAM techniques for developing facial prostheses. Part 1: Design and fabrication of prosthesis replicas. Int J Prosthodont 2003;16:435-441.

COPYRIGHT © 2005 BY QUINTESSENCE PUBLISHING CO, INC.
PRINTING OF THIS DOCUMENT IS RESTRICTED TO PERSONAL USE ONLY.
NO PART OF THIS ARTICLE MAY BE REPRODUCED OR TRANSMITTED IN ANY FORM
WITHOUT WRITTEN PERMISSION FROM THE PUBLISHER.

Copyright of International Journal of Prosthodontics is the property of Quintessence Publishing Company Inc. and its content may not be copied or emailed to multiple sites or posted to a listserv without the copyright holder's express written permission. However, users may print, download, or email articles for individual use.